

# Estimating base resistance and $N$ value in rotary press-in

Yukihiro Ishihara<sup>a,\*</sup>, Stuart Haigh<sup>b</sup>, Malcolm Bolton<sup>b</sup>

<sup>a</sup>Construction Solutions Development Department, Giken Ltd., Japan

<sup>b</sup>Department of Engineering, University of Cambridge, United Kingdom

Received 17 October 2013; received in revised form 5 February 2014; accepted 16 March 2015

Available online 22 July 2015

## Abstract

In the press-in method, press-in machines use static jacking force to install prefabricated piles, while gaining a reaction force by grasping several of the previously installed piles. The emergence of this piling technique in 1975 solved problems in urban piling construction such as noise and vibration associated with the piling work, restricted construction conditions due to the existing structures, and so on. Among a variety of press-in methods, rotary press-in is a relatively new technique to install tubular piles into hard ground by applying axial and rotational jacking force at the same time. An additional feature of the press-in Method is that it allows continuous measurement of penetration depth and jacking force during piling work. The concept of a PPT, Pile Penetration Test, has been developed to apply this feature to improving the efficiency of piling work and foundation design. This paper highlights the technique to estimate base resistance and  $N$  value from the data acquired during rotary press-in.

© 2015 The Japanese Geotechnical Society. Production and hosting by Elsevier B.V. All rights reserved.

**Keywords:** Rotary press-in; Base resistance;  $N$  value

## 1. Introduction

The press-in method is a technique to install piles with a static jacking force. It mitigates the environmental problems of noise and vibration that have been associated with other conventional piling techniques using percussive or vibratory hammers.

This piling method has high spatial efficiency; since a press-in piling machine gains a reaction force from the previously installed piles, there is no need for bulky weights that occupy a large space. This feature is emphasized in the ‘GRB (Giken Reaction Base) System’, where a press-in machine and its

related devices (power unit, pile pitching crane and pile transporter) are all positioned and ‘walk’ on top of the pile wall.

Rotary press-in is a relatively new technique among a variety of press-in methods, installing piles with teeth on the base by applying axial and rotational jacking force at the same time, as shown in Fig. 1. With the emergence of rotary jacking, the applicability of the press-in method to hard ground conditions has been significantly improved (White et al., 2010; Bond, 2011; Hazla, 2013).

In the press-in method, it is possible to obtain continuous data of penetration depth and jacking force in parallel with the piling work. The concept of the PPT, Pile Penetration Test, has been developed, as shown in Fig. 2, so that the obtained data can adequately be processed and practically used. The data obtained in the ‘press-in construction site’ include penetration depth, vertical or rotational jacking force, press-in rate, rotation

\*Corresponding author.

E-mail addresses: [ishihara@giken.com](mailto:ishihara@giken.com) (Y. Ishihara), [skh20@cam.ac.uk](mailto:skh20@cam.ac.uk) (S. Haigh), [mdb@eng.cam.ac.uk](mailto:mdb@eng.cam.ac.uk) (M. Bolton).

Peer review under responsibility of The Japanese Geotechnical Society.



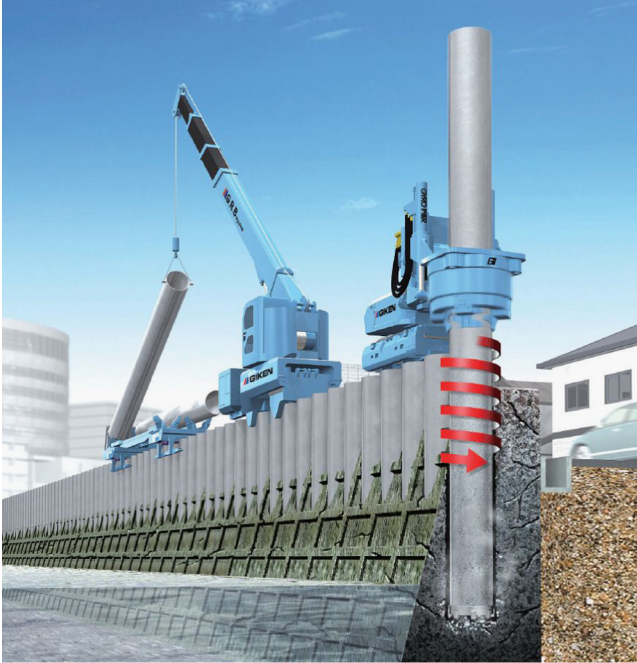


Fig. 1. 'Gyropiler' for rotary press-in, with GRB System.

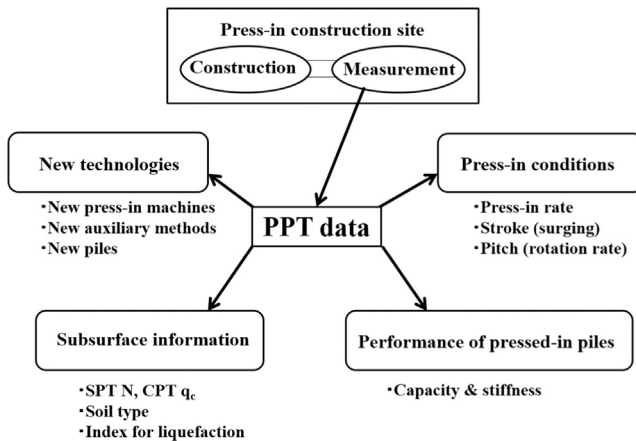


Fig. 2. Concept of 'PPT' – Pile Penetration Test.

rate, and so on, and are called 'PPT data'. Four applications of the PPT data are expected. Operators of a press-in machine will select adequate 'press-in conditions' such as press-in rate and rotation rate based on PPT data; furthermore, a press-in machine will be automatically operated with adequate 'press-in conditions' selected in response to the PPT data. Mechanical engineers will make use of the PPT data to develop 'new technologies' for press-in machines, piles, auxiliary methods and so on. Those who are concerned with the construction process will consult 'subsurface information' estimated from the PPT data, especially when they encounter unexpected ground conditions. Designers interested in how the pressed-in piles perform when they serve as a part of a structure may refer to the PPT data to get some information on the 'performance of pressed-in piles'.

The possibility of estimating subsurface information such as CPT  $q_c$ , SPT  $N$  value and soil type, from PPT data in standard press-in (press-in without any auxiliary methods) has been demonstrated (Ishihara et al., 2009, 2010, 2013). The estimated subsurface information is based on the information of the base resistance during press-in.

Obtaining information of base resistance required a load cell in the pile base to directly measure it until a simple method to estimate it from jacking force was developed by Ogawa et al. (2012). The method postulates a pile to be pressed-in with 'surging', where downward displacement  $l_d$  and upward displacement  $l_u$  are alternately applied to the pile ( $l_d > l_u$ ). Although the method is practical, the information can only be obtained at intermittent depths.

This research proposes and assesses the technique to estimate base resistance, and then  $N$  value, from PPT data during rotary press-in. The technique does not require additional measurement devices other than the existing automatic measurement system in this piling method, and the obtained information will be continuous with depth.

## 2. Estimating base resistance in rotary press-in of closed-ended piles

### 2.1. Estimation method

In rotary jacking, a vertical jacking force and a rotational jacking force (torque) are simultaneously applied to a tubular pile. These jacking forces reflect not only the resistance of a soil on a pile but also forces that are not relevant to the pile–soil interaction, such as the weight of the pile, the weight of a chucking part of the piling machine etc. Excluding these unnecessary forces, it is practical to call the vertical and rotational resistances 'head load' ( $Q$ ) and 'head torque' ( $T$ ) respectively.  $Q$  and  $T$  can be decomposed into a base component (base resistance ( $Q_b$ ), base torque ( $T_b$ )) and a shaft component (shaft resistance ( $Q_s$ ), shaft torque ( $T_s$ )), as expressed in Fig. 3 and Eqs. (1) and (2).

$$Q = Q_b + Q_s \quad (1)$$

$$T = T_b + T_s \quad (2)$$

If we assume the base stress  $q_b$  to be uniformly applied on the base of a closed-ended tubular pile with outer diameter  $D_o$ ,

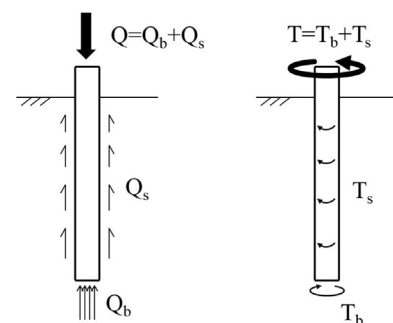


Fig. 3. Decomposition of  $Q$  and  $T$ .



and the coefficient of friction between the soil and the pile base to be  $\tan \delta_{sp}$ , where  $\delta_{sp}$  is the angle of wall friction between the soil and the pile,  $Q_b$  and  $T_b$  can be expressed in the form of

$$Q_b = \frac{\pi D_o^2}{4} q_b \quad (3)$$

$$T_b = \int_0^{D_o/2} \{ (q_b \tan \delta_{sp} 2\pi r dr) r \} = \frac{\tan \delta_{sp} \pi D_o^3}{12} q_b \quad (4)$$

where  $r$  represents the distance from the center of the pile base.

Combining Eqs. (3) and (4), the relationship between  $Q_b$  and  $T_b$  can be expressed as:

$$\frac{2T_b/D_o}{Q_b} = \frac{2 \tan \delta_{sp}}{3} \equiv \xi_C^* \quad (5)$$

If  $\delta_{sp}$  is constant with stress,  $\xi_C^*$  can be assumed to be constant.

In general, the relationship between  $Q_b$  and  $T_b$  will be expressed by the combination of linear and non-linear models, as described by Cassidy and Cheong (2005), Bienen et al. (2007), White et al. (2010) and other researchers. For simplicity, the linear relationship is assumed to derive Eq. (5), which correspondingly expresses the ‘frictional sliding line’ described by Bienen et al. (2007).

Fig. 4 shows how the pile–soil friction ( $f$ ) can be decomposed into vertical and horizontal components, using the index  $\varphi$ , the ratio of the peripheral velocity to the penetration rate. With these two components,  $Q_s$  and  $T_s$  can be expressed in the form:

$$Q_s = \frac{f}{\sqrt{1+\varphi^2}} \pi D_o z \quad (6)$$

$$T_s = \frac{\varphi f}{\sqrt{1+\varphi^2}} \pi z \frac{D_o^2}{2} \quad (7)$$

Assuming  $\varphi$  is constant, Eqs. (6) and (7) provide the relationship between  $Q_s$  and  $T_s$  as:

$$\frac{2T_s/D_o}{Q_s} = \varphi \equiv \xi^* \quad (8)$$

Incorporating Eqs. (1), (2), (5) and (8), the base resistance can be written in the following form:

$$Q_b = \frac{2T/D_o - \xi_C^* Q}{\xi_C^* - \xi^*} \quad (9)$$

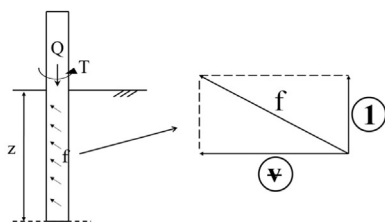


Fig. 4. Decomposition of pile–soil friction  $f$ .

## 2.2. Verification through field testing

A closed-ended tubular pile with  $D_o=318.5$  mm was rotary-pressed-in by a press-in machine known as a ‘Gyropiler’, GRV0615. The site profile is shown in Fig. 5. The test pile was equipped with a base load cell to measure  $Q_b$ . Hydraulic pressures were measured in the press-in machine to obtain  $Q$  and  $T$ . The penetration depth was measured using a stroke sensor connected to the pile head.

Two tests were conducted, as shown in Table 1. The indexes  $v_d$ ,  $v_u$  and  $v_p$  refer to the rate of downward motion of the pile, the rate of upward motion of the pile and the peripheral velocity of the pile respectively. The pile was rotary-pressed-in monotonically (without surging) in C11-10 while rotary-pressed-in with surging in C11-13. Profiles of  $Q$  and  $2T/D_o$  obtained in these tests are shown in Figs. 6 and 7.

The comparison between the ‘measured’  $Q_b$  by the base load cell and the ‘estimated’  $Q_b$  using Eq. (9) is shown in Fig. 8.  $\delta_{sp}$  is assumed as  $17^\circ$  ( $\xi_C^*=0.2$ ), judging from the site profile in

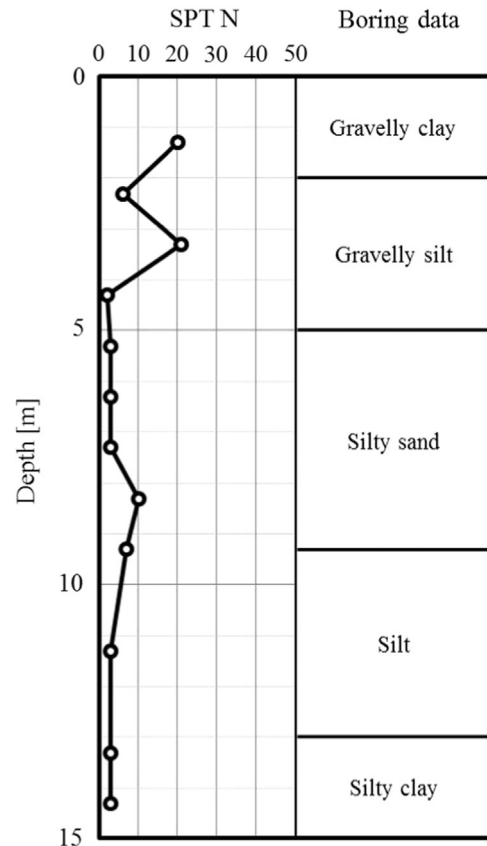


Fig. 5. Site profile.

Table 1  
Press-in conditions in C11 field test.

	$v_d$ [mm/s]	$v_u$ [mm/s]	$v_p$ [mm/s]	$l_d$ [mm]	$l_u$ [mm]
C11-10	23	—	15	800	0
C11-13	23	28	110	800	400



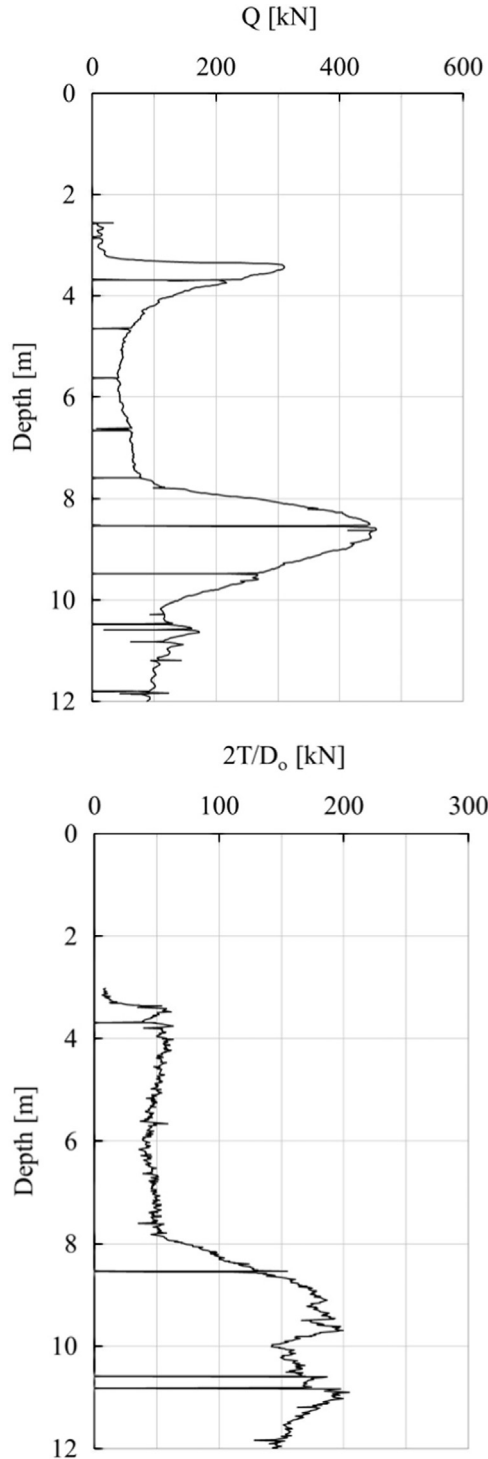
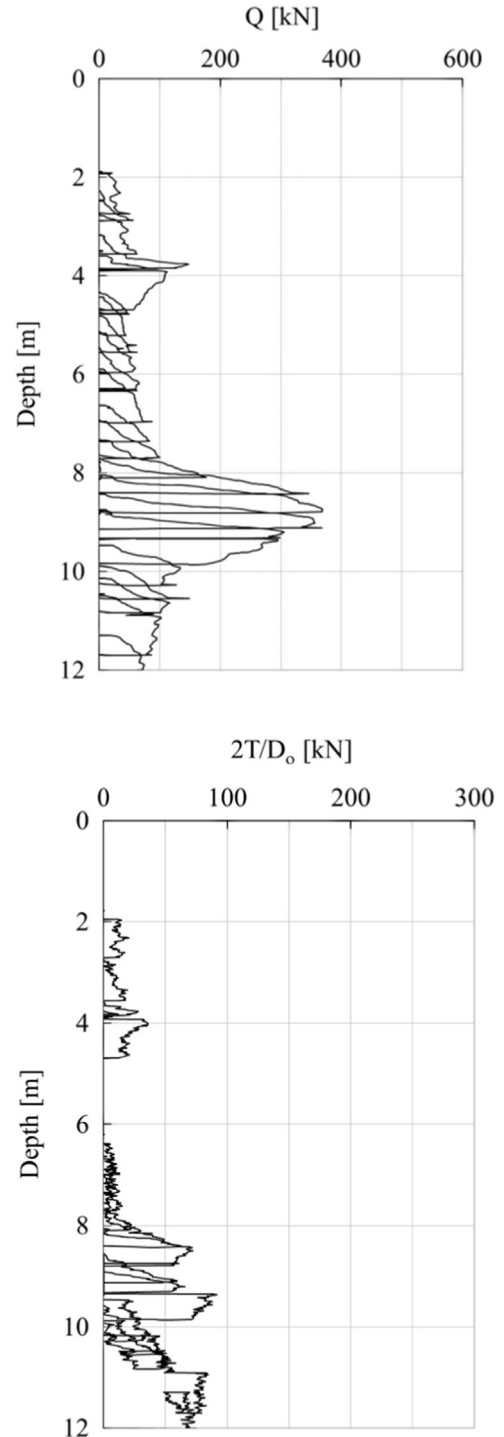
Fig. 6. Profiles of  $Q$  and  $2T/D_o$  in C11-10.

Fig. 5. Good agreement can be found between the measured and estimated  $Q_b$  in both test cases.

### 3. Estimating base resistance in rotary press-in of open-ended piles with teeth on the base

If the pile concerned is an open-ended tubular pile, soil plugging has to be taken into consideration. The condition of

Fig. 7. Profiles of  $Q$  and  $2T/D_o$  in C11-13.

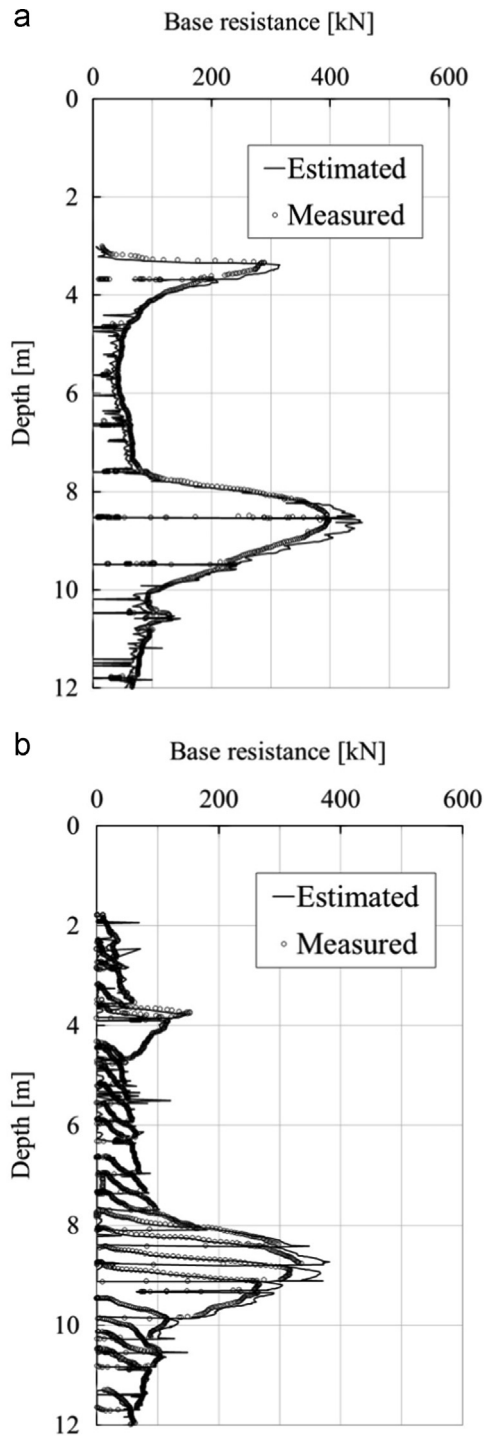
the pile base is not constant during press-in, due to the possible transition between ‘plugged’ and ‘unplugged’ penetration.

A simple index to express this plugging condition is known as IFR, Incremental Filling Ratio (Lehane et al., 2007; White and Deeks, 2007), expressed as follows:

$$IFR = \delta h / \delta z \quad (10)$$

where  $h$  refers to the length of the soil column in the pile. IFR=0 corresponds to a fully plugged condition, IFR=1 a fully



Fig. 8. Comparison of estimated and measured  $Q_b$ .

unplugged condition and  $0 < \text{IFR} < 1$  a partially plugged condition. The plugging condition (the value of IFR) depends on the balance between the resistance of the soil on the bottom of the soil column in the pile ( $Q_{b,\text{in}}$ ) and the sum of the weight of the soil column inside the pile ( $W_s$ ) and the resistance between the soil column and the internal surface of the pile ( $Q_{s,\text{in}}$ ), as shown in Fig. 9, and therefore the variation of  $h$  (or IFR) with depth is not necessarily monotonic. Okada and Ishihara (2012) confirmed this by estimating  $h$  considering the

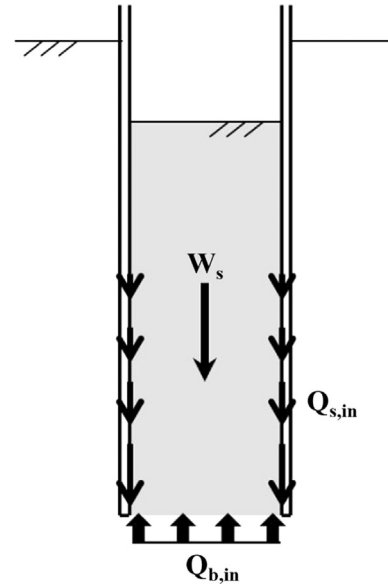
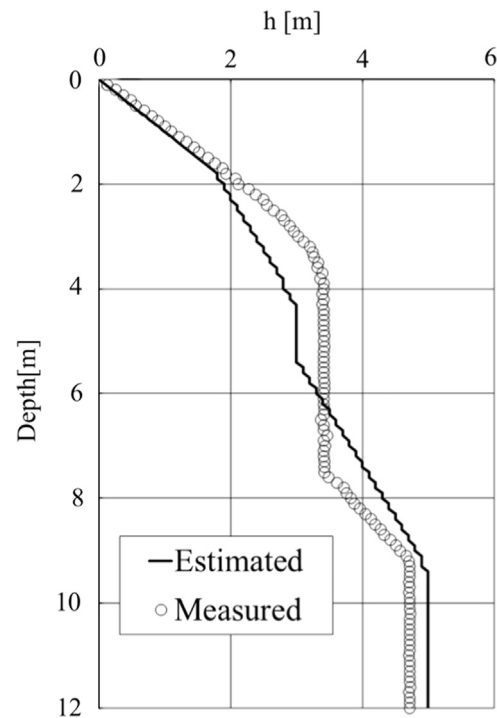


Fig. 9. Forces acting on the soil column.

Fig. 10. Comparison of estimated and measured  $h$ .

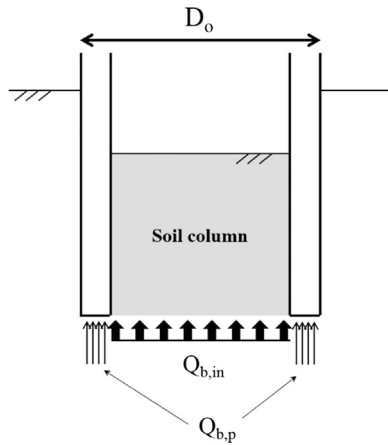
balance of  $Q_{b,\text{in}}$ ,  $W_s$ ,  $Q_{s,\text{in}}$ , which are estimated from the site profile in Fig. 5, and comparing it with the measured  $h$ , as shown in Fig. 10, regarding  $\phi 500$  mm open-ended pile.

For an open-ended pile,  $Q_b$  is the sum of  $Q_{b,\text{in}}$  and the resistance of the soil on the annulus of the pile base ( $Q_{b,p}$ ), as expressed in the following form and in Fig. 11.

$$Q_b = Q_{b,p} + Q_{b,\text{in}} \quad (11)$$

In rotary press-in, the pile is equipped with several teeth on the base to cut the ground.  $Q_{b,p}$  and  $Q_{b,\text{in}}$  could be assumed to



Fig. 11. Decomposition of  $Q_b$  in an open ended pile.

be:

$$Q_{b,p} = t_T w_T n_T q_b \quad (12)$$

$$Q_{b,in} = A_{b,in,eff} q_b \quad (13)$$

$$A_{b,in,eff} = (1 - IFR)(\pi D_{in}^2 / 4) \quad (14)$$

with  $n_T$  being the number of teeth,  $t_T$  and  $w_T$  the thickness and width of each tooth,  $A_{b,in,eff}$  the effective base area inside the pile, and  $D_{in}$  the inside diameter of the pile.

The validity of Eq. (13) can roughly be assessed by comparing its right side with the sum of  $W_s$  and  $Q_{s,in}$ , using the field test data. An open-ended pile with  $D_o = 318.5$  mm and  $D_{in} = 199.9$  mm, equipped with three earth pressure transducers on its base, four pore pressure transducers and four earth pressure transducers on its internal surface, as shown in Fig. 12, was monotonically pressed-in into an alluvial soft soil, with  $v_d = 10$  mm/s.  $Q_{s,in}$  could approximately be estimated as follows:

$$Q_{s,in} = \pi D_{in} \left\{ h_1 \sigma_{h,1}' + \sum_{i=2}^4 (h_i - h_{i-1}) \left( \frac{\sigma_{h,i}' + \sigma_{h,i-1}'}{2} \right) \right\} \tan \delta_{sp} \quad (15)$$

$$\sigma_i' = \sigma_i - u_i \quad (i = 1, 2, 3, 4) \quad (16)$$

where  $h_i$ ,  $u_i$  and  $\sigma_i$  are respectively the height from the pile base, pore water pressure and horizontal earth pressure at the  $i$ -th section from the pile base. As shown in Fig. 13, weak linear correlations can be found in each of the three test cases.

On the other hand,  $T_b$  comprises of the torque to overcome the resistance on the pile base annulus ( $T_{b,p}$ ) and the torque to overcome the resistance at the bottom of the soil column ( $T_{b,in}$ ). Therefore:

$$T_b = T_{b,p} + T_{b,in} \quad (17)$$

With the assumption that  $q_b$  is uniformly applied on the vertical aspect of the teeth (Fig. 14) and on the bottom of the inner soil column,  $T_{b,p}$  can be expressed in the form:

$$T_{b,p} = t_T d_c n_T q_b \frac{D_o + D_{in}}{4} \quad (18)$$

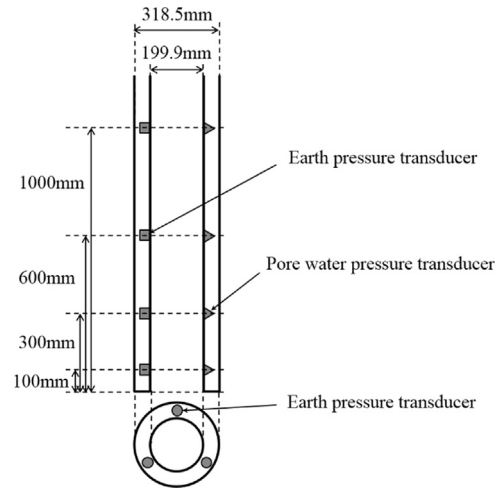


Fig. 12. Schematic illustration of the test pile.

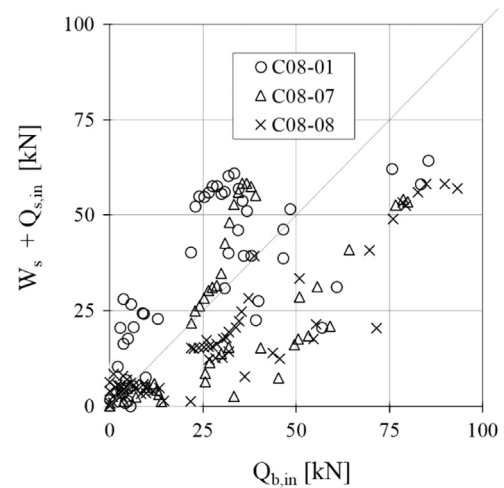
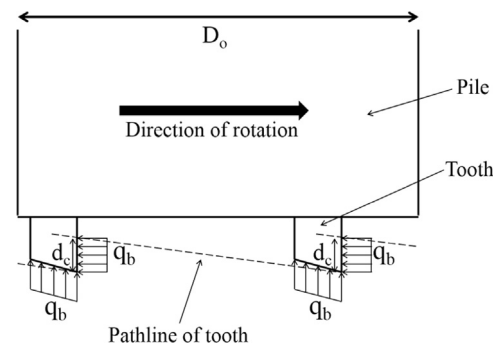
Fig. 13. Correlation between  $W_s + Q_{s,in}$  and  $Q_{b,in}$ .

Fig. 14. Assumption of the resistance on the teeth.

$$d_c = \frac{\pi(D_o + D_{in})}{2n_T \phi} \quad (19)$$

with  $\phi$  being the internal friction angle of soil.



Observation on the surface of the soil column inside the pile with  $D_{in} \approx 780$  mm during rotary press-in in dense sand has shown that it will rotate together with the pile if  $h \geq 0.4D_{in}$ , regardless of the plugging condition in axial direction. Assuming a sliding plane at the bottom of the soil column for simplicity,  $T_{b,in}$  will be expressed as:

$$T_{b,in} = \int_0^{D_{in}/2} \{(1 - IFR)q_b \tan \phi 2\pi r dr\} r \quad (20)$$

Incorporating Eqs. (11)–(14) and (17)–(20), the relationship between  $Q_b$  and  $T_b$  is written as follows:

$$\frac{2T_b/D_o}{Q_b} = \frac{3t_T \pi (D_o + D_{in})^2 + 2\psi(1 - IFR) \tan \phi \pi D_{in}^3}{12\psi n_T t_T w_T D_o + 6\psi(1 - IFR) \pi D_o D_{in}^2} \equiv \xi_{O,T}^* \quad (21)$$

This corresponds to Eq. (5) introduced for closed-ended piles.

By the way, as the relationship between  $Q_s$  and  $T_s$  is irrelevant to the condition at the pile base, Eq. (8) can be applied to their correlation. Therefore, in the same way as Eq. (9) was introduced, the base resistance can be written in the form:

$$Q_b = \frac{2T/D_o - \xi_{O,T}^* Q}{\xi_{O,T}^* - \xi^*} \quad (22)$$

Obtaining information on IFR requires the continuous measurement of  $h$ . If this is difficult, the index of PLR, Plug Length Ratio, which is the ratio of the final length of the inner soil column to the final embedment depth (Xu et al., 2005), can be used in place of IFR. This will deteriorate the accuracy of estimation, especially when  $h$  significantly varies with depth.

## 4. Estimating $N$ value

### 4.1. Estimation method

When a material such as a pile or a CPT cone penetrates into the ground by  $\delta z$ , the soil near the tip of the material has to be removed, displaced or compressed by the corresponding volume  $\delta V$ . This requires a corresponding amount of energy  $\delta E$  to be consumed. In rock drilling, the parameter  $\delta E/\delta V$  is called the specific energy, and has been widely used as the simplest index to specify the mechanical performance of drilling machines (Teale, 1965; Hughes, 1972).

According to Hughes (1972), Li and Itakura (2012), and many other researchers, linear correlation is confirmed between the specific energy in rock drilling and the unconfined compressive strength of rocks. Similarly, a linear correlation is expected between the specific energy in PPT and the  $N$  value, since  $N$  value is the parameter to represent the strength of soil.

The specific energy in rotary press-in ( $(\delta E/\delta V)_{PPT-R}$ ) could be expressed in the following form:

$$\left(\frac{\delta E}{\delta V}\right)_{PPT-R} = \frac{Q_b \delta z + 2\pi n \delta t T_b}{A_{b,eff} \delta z} \quad (23)$$

where  $n$  is the rotational revolution and  $t$  represents time.  $A_{b,eff}$  is the effective base area of the pile, expressed as:

$$A_{b,eff} = \frac{\pi}{4} (D_o^2 - D_{in}^2) + A_{b,in,eff} \quad (24)$$

The specific energy in SPT ( $(\delta E/\delta V)_{SPT}$ ) will be written as follows:

$$\left(\frac{\delta E}{\delta V}\right)_{SPT} = \frac{m_w g h_w e N}{a_{b,eff} \delta z_{SPT}} \quad (25)$$

with  $m_w$  and  $h_w$  being the mass and the drop height of the weight,  $g$  the gravitational acceleration,  $e$  the energy efficiency,  $a_{b,eff}$  the effective base area of the sampler and  $\delta z_{SPT}$  the reference penetration of the SPT ( $=0.3$  m). The equation indicates that  $(\delta E/\delta V)_{SPT}$  is proportional to  $N$ . Therefore, a linear correlation can be expected between  $(\delta E/\delta V)_{SPT}$  and  $(\delta E/\delta V)_{PPT-R}$ :

$$\left(\frac{\delta E}{\delta V}\right)_{PPT-R} = \chi \left(\frac{\delta E}{\delta V}\right)_{SPT} \quad (26)$$

with  $\chi$  being the constant representing the relative efficiency of pile penetration in terms of energy consumption. If the penetration process consumes unnecessary energy, the value of  $\chi$  should be greater than 1. The unnecessary energy consumption is typically attributed to too much extraction (inadequately large value of  $l_u$ ) and too much rotation (inadequately large value of  $\psi$ ).

Combining Eqs. (23)–(26) gives the following:

$$N = \frac{a_{b,eff} \delta z_{SPT} (Q_b \delta z + 2\pi n \delta t T_b)}{\chi m_w g h_w e A_{b,eff} \delta z} \quad (27)$$

### 4.2. Verification through field testing

Three series of field tests were conducted in Kochi, Japan, to confirm the validity of Eq. (27). The pile configurations and press-in conditions are shown in Tables 2 and 3 respectively. The index  $f_w$  refers to the flow rate of the water injected at the pile base. The actual values of  $v_d$ ,  $v_u$  and  $v_r$  may sometimes be

Table 2  
Configuration of piles.

	$D_o$ [mm]	$D_{in}$ [mm]	$n_T$ [mm]	$t_T$ [mm]	$w_T$ [mm]
J1001	800	776	6	40	65
C12	800	776	4	40	65
J1404	1000	976	6	40	65

Table 3  
Press-in conditions in the field tests.

	$v_d$ mm/s	$v_u$ mm/s	$v_p$ mm/s	$Q_{max}$ kN	$T_{max}$ kNm	$l_u$ mm	$f_w$ l/min
J1001-1	12–16	22	240	400	—	60	30
J1001-4	12	22	240	500	—	40	30
C12-21	8	6	150	600	—	40	90
C12-22	8	18	110	600	—	40	90
J1404-5	10	30	340	600	500	40	60



smaller than the values in the table, especially when the piling machine needs to generate large  $Q$  or  $T$ .  $Q_{\max}$  and  $T_{\max}$  in the table are not the capacity of the machine but the manually-set limitations. Once  $Q$  or  $T$  reaches these limitations, the pile is extracted by  $l_u$ .

J1001 series were conducted near a river. As shown in Fig. 15, the test site is multi-layered and inhomogeneous, especially 3–8 m below the ground level, due to the transition of the river channel over a long period of time. Fig. 16 is showing the PPT results; the  $N$  values estimated from the data in rotary press-in in this site. Here,  $\chi=1$  was assumed, and PLR was adopted instead of IFR. It can be said that PPT provides similar results with SPT;  $N$  values vary around 10 or 15 in  $0 < z < 10$  and sharply increase to over 30 in  $10 < z < 12$ . Looking at Fig. 15 in detail, differences can be found in the four SPT results in  $5 < z < 9$ . This will be mainly reflecting the effect of the existence of gravels, judging from the information of the boring data in Fig. 15. On the other hand, the  $N$  values confirmed by PPT in the corresponding depths are relatively consistent with each other and smaller than the SPT results, as can be seen in Fig. 16. The reason for this can be surmised that gravels did not exist in the corresponding depths at the two points of PPT, or that PPT is less sensitive to the same size of gravels compared with SPT, because of the greater size of the penetrating material;  $D_o=800$  mm for PPT in this case while the outer diameter of the penetrating sampler in SPT is around 50 mm.

C12 and J1404 series were carried out near a seashore. The site profiles are shown in Fig. 17. The site consists of two layers (sand and sandy gravel), and the both layers are dense, judged from the  $N$  values in the figure. Fig. 18 is showing the PPT results; the  $N$  values estimated from the data in rotary press-in in this site. Again,  $\chi=1$  was assumed, and PLR was adopted instead of IFR. SPT and PPT results are roughly comparable, in that  $N$  values gradually increase to 50 with depth in  $0 < z < 8$  and that they become greater than 50 at

several depths in  $10 < z < 12$ . Significantly large values are found at 8.5 m in C12-22 and at 7 m in J1404-5. These have been confirmed to be due to the large values of  $l_u$  (approximately 500 mm in both cases), which were irregularly necessary to improve (recover) the efficiency of penetration. Some of the  $N$  values in  $8 < z < 12$  are also significantly large (as large as 100). This is presumably because the ground condition at these points was actually hard, or because of the negative effect of the use of PLR in place of IFR on the estimated values. The values of PLR in the three tests were 0.7, 0.74 and 0.7. If IFR is assumed as 0.3 and is used instead of these PLR values, for example, the estimated  $N$  values reduce to 61 at

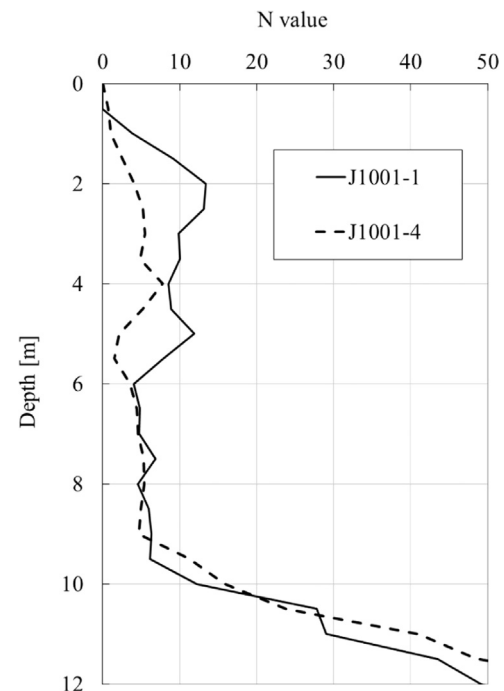


Fig. 16. PPT results in J1001.

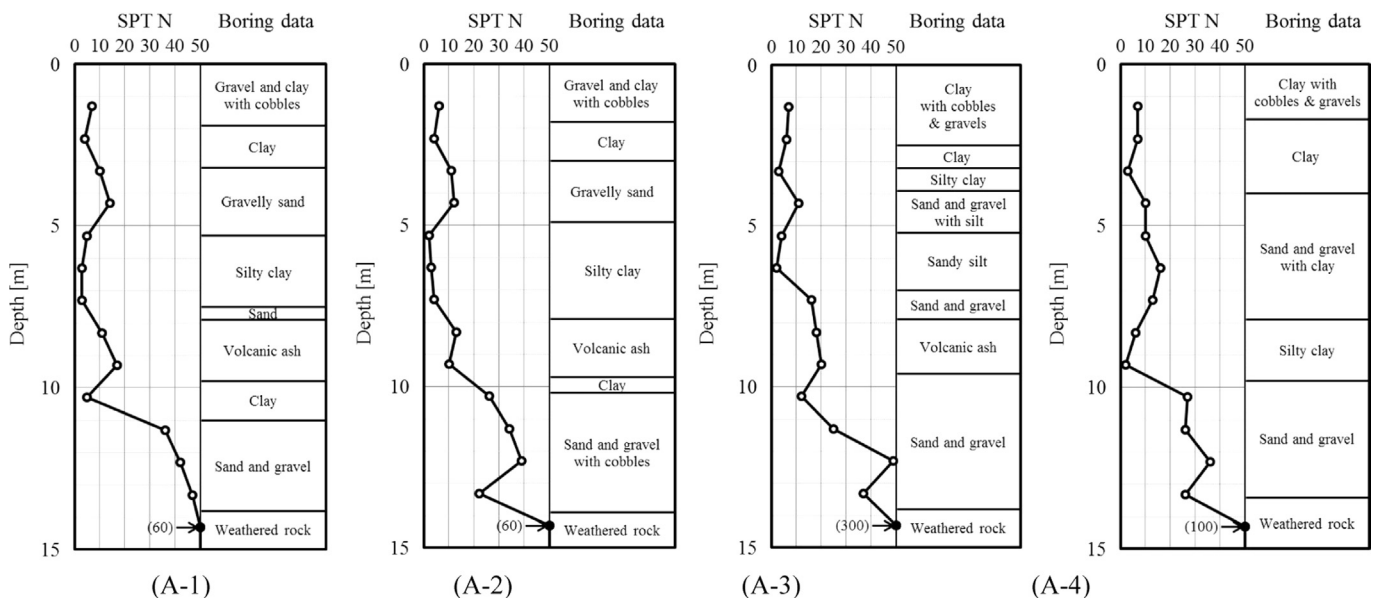


Fig. 15. Site profiles in J1001 field test.



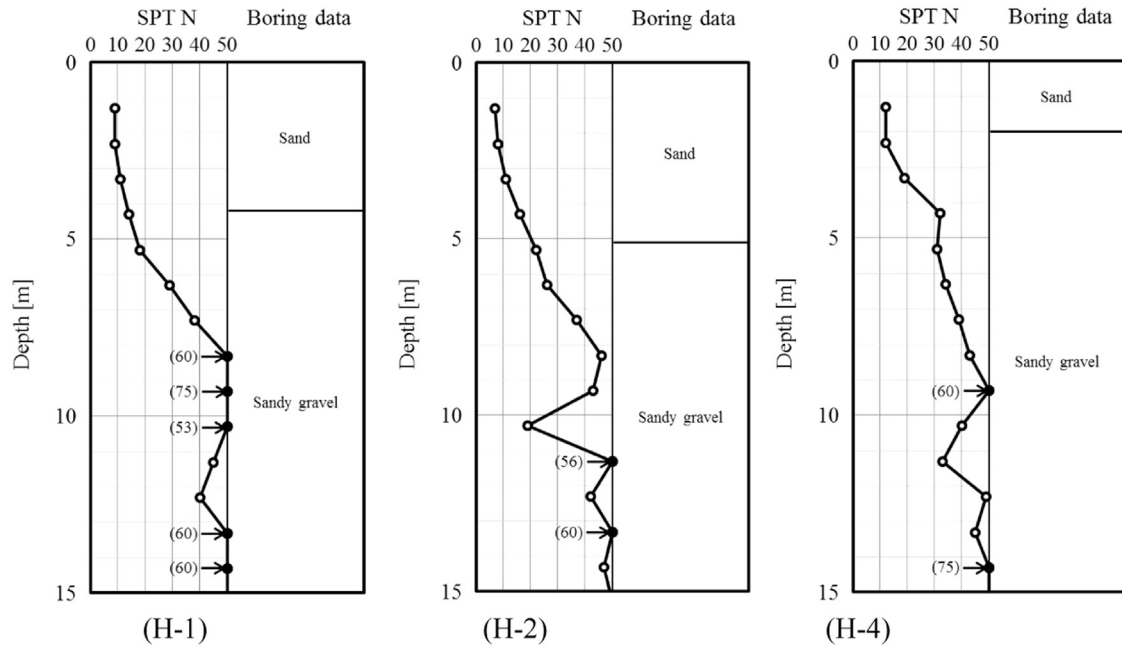


Fig. 17. Site profiles in C12 and J1404 field test.

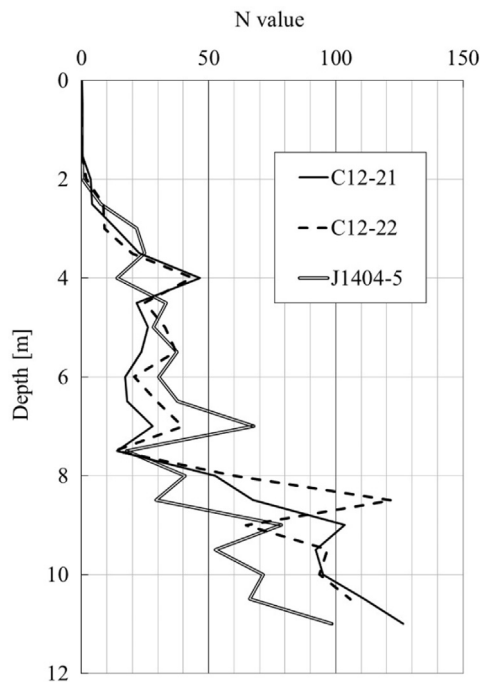


Fig. 18. PPT results in C12 and J1404.

11 m for C12-21, 40 at 10 m for C12-22 and 46 at 11 m for J1404-5. Accurate information of IFR, which requires continuous measurement of  $h$ , is essential for the reliability of the PPT results.

## 5. Conclusions

A method to estimate base resistance during rotary press-in was proposed for closed ended piles. The method does not require additional measurement devices other than the

conventionally used automatic data acquiring system in this piling technique, and provides information that is continuous with depth. Good agreement was confirmed between the estimated and measured base resistance.

This method was then extended to open-ended piles with teeth on the base, and the estimated base resistance was converted to SPT  $N$  value through the comparison of the specific energy in SPT and rotary press-in (PPT). Field test results showed that PPT results roughly represent SPT  $N$  values. The differences between PPT and SPT results were assumed to be attributed to one of the following: (1) the actual difference in the ground condition at the points of PPT and SPT, (2) the difference in the sensitivity to large gravels, or, (3) limited information of the length of the inner soil column in PPT.

## References

- Bienen, B., Gaudin, C., Cassidy, M.J., 2007. Centrifuge tests of shallow footing behavior on sand under combined vertical – torsional loading. *Int. J. Phys. Model. Geotech.* 2 7 (2), 1–21.
- Bond, T., 2011. Rotary jacking of tubular piles (M.Eng. Project Report). Cambridge University Department of Engineering, 50 pp..
- Cassidy, M.J., Cheong, J., 2005. The behavior of circular footings on sand subjected to combined vertical – torsion loading. *Int. J. Phys. Model. Geotech.* 5 (4), 1–14.
- Hazla, E., 2013. Rotary Press-in in Hard Ground (M.Eng. Project Report). Cambridge University Department of Engineering, 50 pp..
- Hughes, H.M., 1972. Some aspects of rock machining. *Int. J. Rock Mech. Min. Sci.* 9, 205–211.
- Ishihara, Y., Ogawa, N., Kinoshita, S., Tagaya, K., 2009. Study on soil classification and  $N$  value based on PPT data. Symposium on Recent Sounding Technologies and Assessment of Ground conditions. pp. 85–90 (in Japanese).
- Ishihara, Y., Nagayama, T., Tagaya, K., 2010. Interpretation of PPT data for more efficient pile construction. In: Proceedings of the 11th International



- Conference on Geotechnical Challenges in Urban Regeneration. London, UK, CD.
- Ishihara, Y., Ogawa, N., Lei, M., Okada, K., Nishigawa, M., Kitamura, A., 2013. Estimation of  $N$  value and soil type from PPT data in standard press-in and press-in with augering. In: *Press-in Engineering 2013: Proceedings of 4th IPA International Workshop in Singapore*. pp. 116–129.
- Lehane, B.M., Schneider, J.A., Xu, X., 2007. CPT-based design of displacement piles in siliceous sands, *Advances in Deep Foundations* 69–86.
- Li, Z., Itakura, K., 2012. An analytical drilling model of drag bits for evaluation of rock strength. *Soils Found.* 52 (2), 206–227.
- Ogawa, N., Nishigawa, M., Ishihara, Y., 2012. Estimation of soil type and  $N$ -value from data in press-in piling construction. *Testing and Design Methods for Deep Foundations*. IS-Kanazawa, 2012; 597–604.
- Okada, K., Ishihara, Y., 2012. Estimating bearing capacity and jacking force for rotary jacking. *Testing and Design Methods for Deep Foundations*. IS-Kanazawa, 2012; 605–614.
- Teale, R., 1965. The concept of specific energy in rock drilling. *Int. J. Rock Mech. Min. Sci.* 2, 57–73.
- White, D.J., Deeks, A.D., 2007. Recent research into the behaviour of jacked foundation piles, *Advances in Deep Foundations* 3–26.
- White, D.J., Deeks, A.D., Ishihara, Y., 2010. Interpretation of PPT data for more efficient pile piling: axial and rotary jacking. In: *Proceedings of the 11th International Conference on Geotechnical Challenges in Urban Regeneration*, London, UK, CD.
- Xu, X., Lehane, B.M., Schneider, J.A., 2005. Evaluation of end-bearing capacity of open-ended piles driven in sand from CPT data. In: *Proceedings of the International Symposium on Frontiers in Offshore Geotechnics*. pp. 725–731.